applied sciences

MDPI

Article

Pressure–Relief Gas Cooperative Drainage Technology in a Short-Distance Coal Seam Group

Lianqin Ni [1], Anying Yuan [1,*] and Zuxiang Hu [2]

[1] State Key Laboratory of Mining Response and Disaster Prevention and Control in Deep Coal Mine, Anhui University of Science and Technology, Huainan 232001, China
[2] College of Safety Science and Engineering, Anhui University of Technology, Huainan 232001, China
* Correspondence: ayyuan@aust.edu.cn

Abstract: The gas in a coal seam is a clean energy source, but it is also the main cause of gas accidents during the mining of mineral resources. There is a large pressure–relief gas influx in the upper and lower adjacent layers of 1211 working face in the Wanfeng Coal Mine in Jinhui, Shanxi Province, China. Based on the evolution law of overburden fractures, the collaborative pressure–relief gas extraction mode of "directional drilling in the gas-conducting fractured zone + staggered buried-pipe in the goaf" is innovatively proposed. The research results indicate that, under the influence of gas pressure gradient and buoyancy, a gas–concentration enrichment zone is formed at a distance of 10.8–24.1 m from the boundary of the mining layer. After optimizing the arrangement of roof directional-drilling layer and layer position, as well as the staggered distance of buried pipe drainage, the average gas-drainage rate reached 83.2% during the test working face, and the gas volume fraction in the upper corner was maintained below 0.7%. This mode can greatly improve the efficiency of mining mineral resources and gas energy utilization in short-distance coal seam groups, while solving the problem of gas accumulation in the upper corner caused by negative pressure of air flow during the mining process of mineral resources.

Keywords: short-distance coal seam group; fracture development; gas energy utilization; cooperative extraction; optimal design

check for updates

Citation: Ni, L.; Yuan, A.; Hu, Z. Pressure–Relief Gas Cooperative Drainage Technology in a Short-Distance Coal Seam Group. *Appl. Sci.* **2023**, *13*, 5534. https://doi.org/10.3390/app13095534

Academic Editor: Daniel Dias

Received: 2 March 2023
Revised: 25 April 2023
Accepted: 27 April 2023
Published: 29 April 2023

Copyright: © 2023 by the authors. Licensee MDPI, Basel, Switzerland. This article is an open access article distributed under the terms and conditions of the Creative Commons Attribution (CC BY) license (https://creativecommons.org/licenses/by/4.0/).

1. Introduction

China's gas disasters are extremely severe [1]. Ninety-five percent of high-gas mines are in low-permeability coal seams, and the adsorbed gas content accounts for more than 80% [2,3]. In a high-gas coal seam group, protective layer mining, combined with pressure–relief gas extraction, is the most economical and effective measure for gas disaster prevention and control [4–6]. However, with coal seam spacing of less than 10 m, no matter which layer is selected as the first mining protective layer, the adjacent layers are all in the pressure–relief range [7,8]. The gas in the pressure–relief state has the characteristics of a large desorption amount and a fast desorption speed [9]. Under the combined action of gas pressure and the negative pressure of ventilation, the pressure-relieved gas flows through overburden fractures to the mining layer [10]. At present, pressure–relief gas extraction is an effective technical measure to control gas in short-distance coal seam groups.

Scholars have undertaken considerable research into the pressure–relief gas treatment technology of short-distance coal seam groups. Cui [11] studied the evolution law and distribution characteristics of overburden fractures for repeated mining in short-distance seam groups. Using numerical simulation, Yang [12] studied stress evolution and nonlinear action after multiple depressurization mining in short-distance seam groups. Wang [13] analyzed the gas permeation evolution mechanism of coal seam mining and proposed a comprehensive extraction technology. Cheng [14] studied the treatment technology of stress release gas in short-distance seam groups using physical experiments. Lin [15] and Lu [16]

proposed the technology of pressure–relief gas extraction using large diameter boreholes. Gao [17] and Hu [18] studied the permeability-increasing effect of high-level drainage roadways in the process of coal seam group mining. An [19] and Duan [20] investigated the effect of pressure–relief gas drainage from adjacent seams using high-level boreholes and field tests. Saba Gharehdash [21] developed RCPNMs to calculate the topology and geometry properties of explosively created fractures.

In summary, predecessors have adopted high drainage roadways, roof (floor) plate drilling, roof high (low) drillings, and goaf buried-pipe extraction methods for gas control, depending on the coal seam occurrence conditions and technical processes. Their research results have provided theoretical and technical support for gas prevention and control of short-distance coal seam groups. However, many problems have not yet been fully resolved. Although the extraction volume of a high drainage roadway is large, it also requires much engineering work and is expensive. Furthermore, the perforation speed of the top (bottom) plate is rapid, but it is difficult to maintain the drilling. Moreover, although the layout of the buried-pipe extraction is flexible, and the investment costs are low, the position of the buried-pipe orifice can be affected, resulting in the disadvantage of a poor extraction effect.

The existing research on gas control in short-distance coal seam groups has focused on the determination of single technical parameters. The layout parameters of pressure–relief gas extraction holes in adjacent strata mostly depend on field measurements or empirical formula estimation of the height of the "three-vertical zones" of traditional strata movement. When the influence of the difference in overburden structures of short-distance coal seam groups on gas migration and the enrichment of the adjacent seams is ignored, it becomes clear that the research into gas control measures and the determination of specific parameters is not sufficiently comprehensive. In this paper, the 1211 working face of Shanxi Jinhui Wanfeng Coal Mine was taken as the research object. Due to the pressure–relief gas influx in the mining layer, it is difficult to simultaneously control the gas emissions of the upper and lower adjacent layers with a single extraction measure. The characteristics of gas pressure–relief migration and enrichment in adjacent layers are analyzed based on the "three zones" theory of gas relief migration. This in-depth study of the spatial coupling relationship of pressure–relief gas treatment measures innovatively proposes the "directional long drilling in the gas-conducting fractured zone + staggered buried-pipe in the goaf" drainage pressure–relief gas cooperative technology, and it investigates the effect of pressure–relief gas treatment. The results demonstrate an effective improvement in the efficiency of mineral resource mining and gas energy utilization in short-distance coal seam groups.

2. Fracture Evolution Mechanism of the First Mining Layer in the Short-Distance Coal Seam Group

In the mining conditions of the short-distance coal seam group, the roof and floor of coal seam are displaced and deformed, generating cracks and forming gas migration channels. Based on the slip-line field theory, the coal and rock mass in a certain range under the stope floor lies in the stress cross area [22,23]. Under the action of shear stress, the floor coal and rock mass in the stress reduction area is easily further damaged in the edge area of the coal pillar and produces mining fissures. The supporting pressure range moves continuously with the advance of the working face. The damaged coal and rock mass moves to the goaf under the action of extrusion pressure, and the goaf floor expands to form a continuous sliding surface, as shown in Figure 1. At the same time, under the influence of ore pressure, the floor coal and rock mass are periodically destroyed, and the permeability is further increased. The pressure–relief gas of the underlying coal seam rises to the stopping layer along the fracture network through diffusion and seepage.

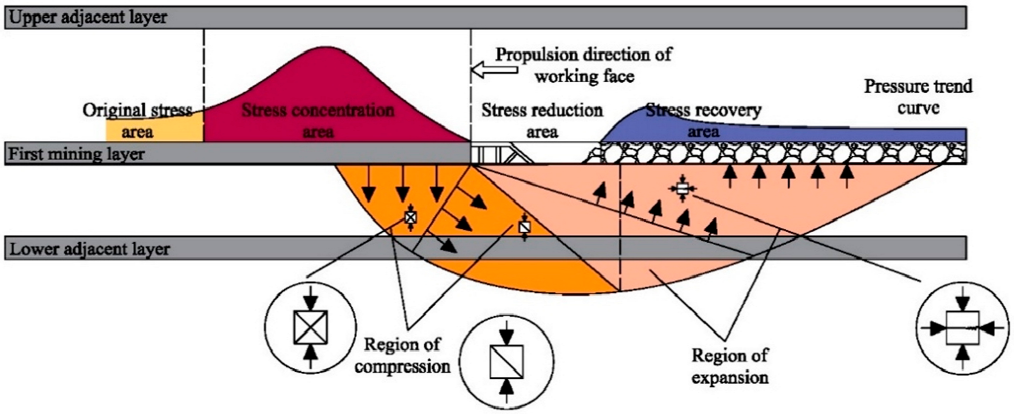

Figure 1. Stress field and fracture distribution of mining floor in the first mining layer of the short-distance coal seam group.

In the short-distance coal seam group, the underlying coal seam close to the goaf expands and deforms due to full pressure–relief, and the underlying coal seam fracture is fully developed. The horizontal bed separation fractures and vertical broken fractures are connected with the primary fractures of the coal and rock mass to form the main channel of pressure–relief gas migration. Under the actions of rising and the pressure gradient, the relieved gas migrates to the mining seam through the fracture network, which increases the difficulty of gas management at the working face of the first mining layer.

In the short-distance coal seam group, there is an obvious inflection point in the deformation and displacement of the roof strata. The upper and lower bearing surfaces of the rock stratum in front of the inflection point bear tensile and compressive stresses, respectively, and the upper and lower bearing surfaces of the rock stratum at the rear bear compressive and tensile stresses, respectively. Due to the heterogeneity of the rock strata, the ultimate tensile and compressive strengths of the rock masses within and between the rock strata are different. When the tensile and compressive stresses exceed the ultimate tensile and compression strengths of rock masses, there must be a transverse and longitudinal fracture network, as shown in Figure 2. Based on the co-mining theory of coal and gas, combined with the migration characteristics of pressure-relieved gas in the "three-vertical zones", the overlying coal strata of the first mining seam in the short-distance coal seam group is divided into a "gas-conducting fracture zone", "pressure-relieved desorption zone", and "difficult desorption zone" [24]. There is a fracture network consisting of fractures along the seam and broken fractures in the gas-conducting fracture zone [25]. The gas in the adjacent seam can be fully relieved and flows into the mining seam. The gas in this area can be fully exploited, and its height is related to the location of the key seam [26,27].

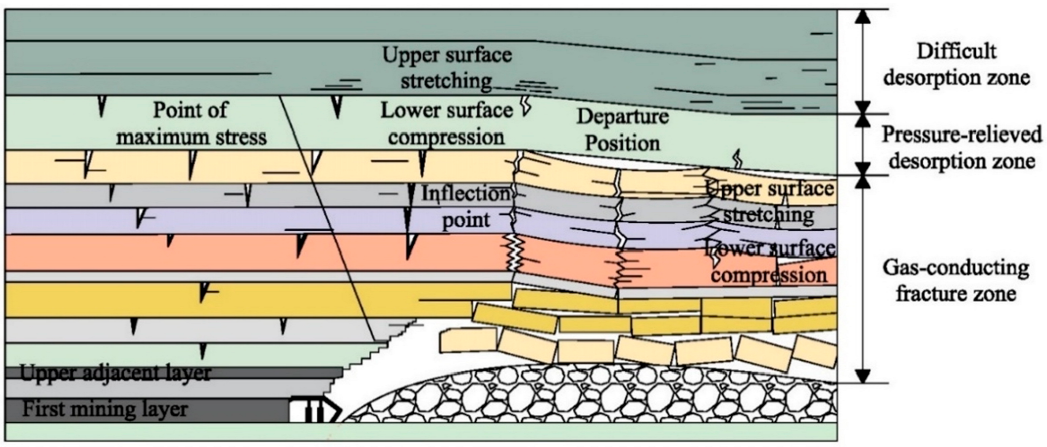

Figure 2. Stress and deformation of the roof in the short-distance seam group.

The spacing of overlying strata on the first mining layer of the short-distance coal seam group is small, and the occurrence conditions of coal strata are complicated. Under the disturbance of mining, the distribution of surrounding rock stress and overlying rock fracture is more complex, the deformation and failure of the coal and rock mass are more serious, the pressure–relief of mining is more sufficient, and the difficulty of gas management is increased.

3. Gas Migration and Enrichment Characteristics of Pressure–relief Gas in the First Mining Seam of the Short-Distance Coal Seam Group

3.1. Engineering Background

Shanxi Jinhui Wanfeng Coal Mine is located approximately 10 km southwest of Xiaoyi City, Shanxi Province, China. The topographic map of Wanfeng Coal Mine is shown in Figure 3. The No. 1-2 coal seam is mined at the 1211 working face, the average thickness being 1.5; the average buried depth is 540 m, and the gas content is 10.66 m^3/t, and the gas pressure is 0.65 MPa. The permeability coefficient of the coal seam is 1.9358 $m^2/(MPa^2 \cdot d)$. The average distance between the No. 1-1 coal seam and the No. 1-2 coal seam is 5.5 m, and the average thickness of the No. 1-1 coal seam is 0.64 m. The No. 1-1 coal seam belongs to the sporadic minable coal seam. The gas content is 9.71 m^3/t, gas pressure is 0.62 MPa, and coal seam permeability coefficient is 0.3492 $m^2/(MPa^2 \cdot d)$. The average distance from the No. 2 coal seam to the No. 1-2 coal seam is 6.95 m, and the average thickness of the No. 2 coal seam is 0.74 m. The No. 2 coal seam is unmineable. The gas content is 14.36 m^3/t, the gas pressure is 0.66 MPa, and the permeability coefficient of the coal seam is 0.5698 $m^2/(MPa^2 \cdot d)$. The rock column diagram is shown in Figure 4. The design strike length of the working face is 870 m, the inclination length is 170 m, and the average dip angle of the coal seam is 4°. U-shaped ventilation has been adopted.

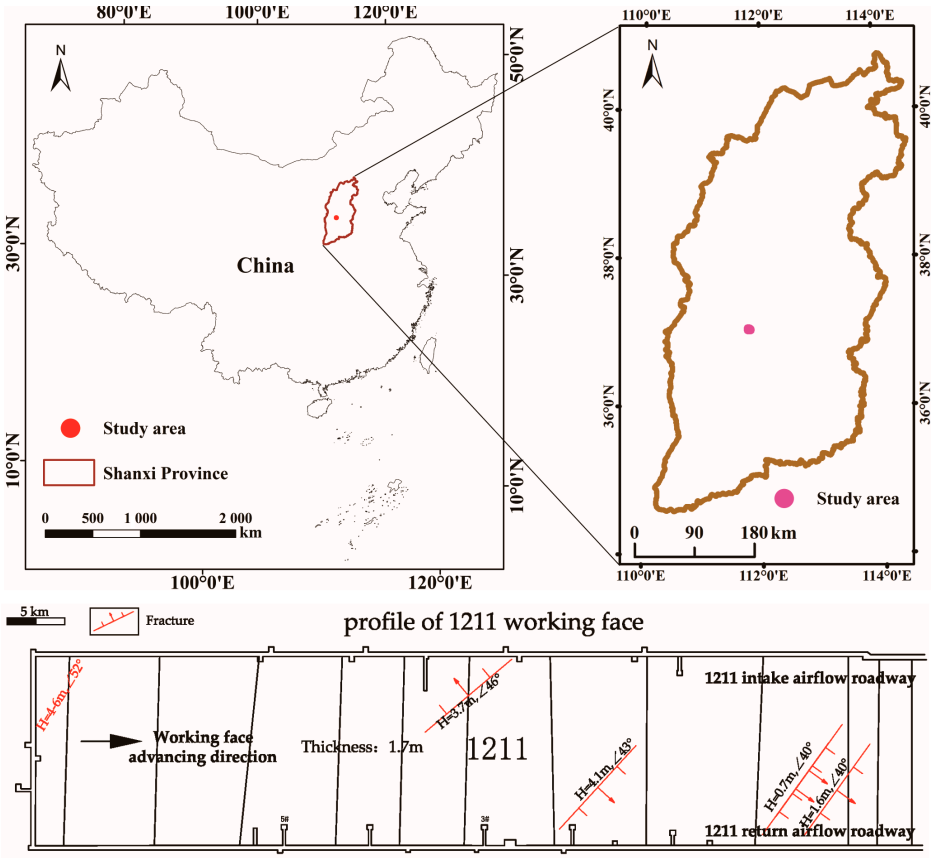

Figure 3. The Wanfeng Coal Mine topographic map.

Stratigraphic units			Thickness(m)			Lithological column 1:500	Lithological descriptin
Erathem	System	Serirs	Group (m)	Total (m)	Layer (m)		
Paleozoic	Permian	Low series	43.3 m	442.22 m	3.50 m		Bauxite mudstone
				445.72 m	4.40 m		Medium sandstone and coarse sandstone
				450.12 m	4.80 m		Mudstone
				454.92 m	5.40 m		Coarse sandstone
				460.32 m	12.60 m		Sandy mudstone
				472.92 m	12.60 m		Coarse sandstone
			44.8 m	485.52 m	10.20 m		Sandy mudstone
				495.72 m	12.10 m		Coarse sandstone and mudstone
				507.82 m	8.30 m		Coarse sandstone
				516.12 m	10.20 m		Sandy mudstone
				526.32 m	4.00 m		Medium sandstone and coarse sandstone
			30.70 m	530.32 m	3.50 m		Sandy mudstone
				533.82 m	0.68 m		No. 1-1 coal seam
				534.50 m	5.50 m		Sandy mudstone and coarse sandstone
				540.00 m	1.50 m		No. 1-2 coal seam
				541.50 m	6.95 m		Medium sandstone and coarse sandstone
				548.45 m	0.74 m		No. 2 coal seam
				549.19 m	1.40 m		Mudstone
				550.59 m	10.38 m		Sandy mudstone

Figure 4. Coal seam histogram.

3.2. Physical Model Establishment and Parameter Setting

Taking the 1211 working face as the prototype, the gas flow in the goaf was simplified into a steady-state flow field, ignoring the influence of personnel and supports. COMSOL was used to construct the goaf data model. The calculation model simplified the working face, intake, and return air roadways as cuboids. The length of the working face was 170 m, and the height was 2.5 m. The distance from the rear boundary of the goaf calculation area to the working face was set to 200 m, the width of the inlet and return air roadway was 4 m, and the height was 2.5 m. The model was divided into multiple regions according to the different permeabilities. The middle of the goaf was the compaction zone, and the surrounding area was the "O" ring. The compaction zone and the "O" ring were divided into four regions from top to bottom; these included the upper part of the fracture zone. The lower part of the fracture zone, the upper part of the caving zone, and the bottom of the caving zone were investigated. The "O" ring was subdivided into 16 regions from front, back, left, and right. It was assumed that the permeability coefficients of each region were anisotropic and uniformly distributed. The grid was encrypted and divided into 410,000 units, as shown in Figure 5.

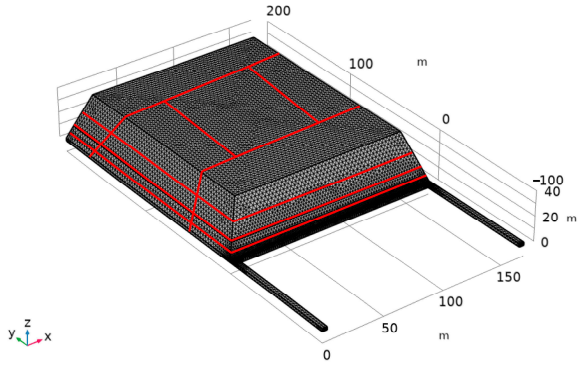

Figure 5. Stope model diagram.

Three important parameters, permeability, porosity, and gas source term, were determined in the COMSOL simulation of the gas flow process in the mining fracture field. The permeability coefficient and porosity of the goaf are related to the coefficient of rock collapse and crushing expansion, and they follow the Blake-Kozeny formulas, Formulas (1) and (2):

$$k = \frac{\varepsilon^3 d_m^2}{150(1-\varepsilon)^2} \tag{1}$$

$$\varepsilon = 1 - \frac{1}{K_P} \tag{2}$$

k—permeability coefficient;
ε—porosity;
Kp—coefficient of dilatancy of crushed stone;
dm—average particle diameter of porous media, m.

The gas quality sources in the model are set as the gas source of the coal wall, the residual coal in the goaf, and the gas emission source of the adjacent seam. According to the field measurement, the gas emission from the coal wall of the 1211 working face was 5.3 m^3/min, and the gas emission from the residual coal in the goaf and the upper and lower adjacent seams was 19.3 m^3/min. The gas emission in the model was regarded as continuous; that is, the gas sources in each area were averaged to the unit volume of the calculation domain, and the gas emission source of each area was determined according to Formula (3):

$$Q_S = \frac{Q_g \cdot \rho_g}{V} \tag{3}$$

Q_s—model gas mass source term, kg/($m^3 \cdot s^{-1}$);
Q_g—gas emission, m^3/s;
ρ_g—gas density, 0.7167 kg/m^3;
V—total volume of the gas mass source term, m^3.

The position of the intake air roadway was set as the speed boundary; the wind speed was 2 m/s, and the gas concentration was 0. The return air roadway was the outlet boundary and was set to free outflow type; the remaining solid boundaries were set to the wall surface. The parameter values of this model are shown in Table 1.

Table 1. Relevant parameter values for different regions.

Region	Natural Accumulation Area	Load Influence Zone	Recompaction Zone	Coal wall Influence Area	Compaction Stable Zone
Crushing expansion coefficient	1.20	1.12	1.05	1.13	1.08
Porosity/%	0.17	0.11	0.05	0.12	0.07
Permeability/m^2	1.45×10^{-11}	1.20×10^{-11}	0.03×10^{-11}	0.30×10^{-11}	0.14×10^{-11}

3.3. Research on the Pressure–Relief Gas Migration Law of Short-Distance Coal Seam Group

The numerical simulation was performed according to the established numerical model and parameter settings until the calculation results converged. The simulation diagrams of the goaf gas distribution law for the mining of No. 1-2 coal seam are shown in Figure 6.

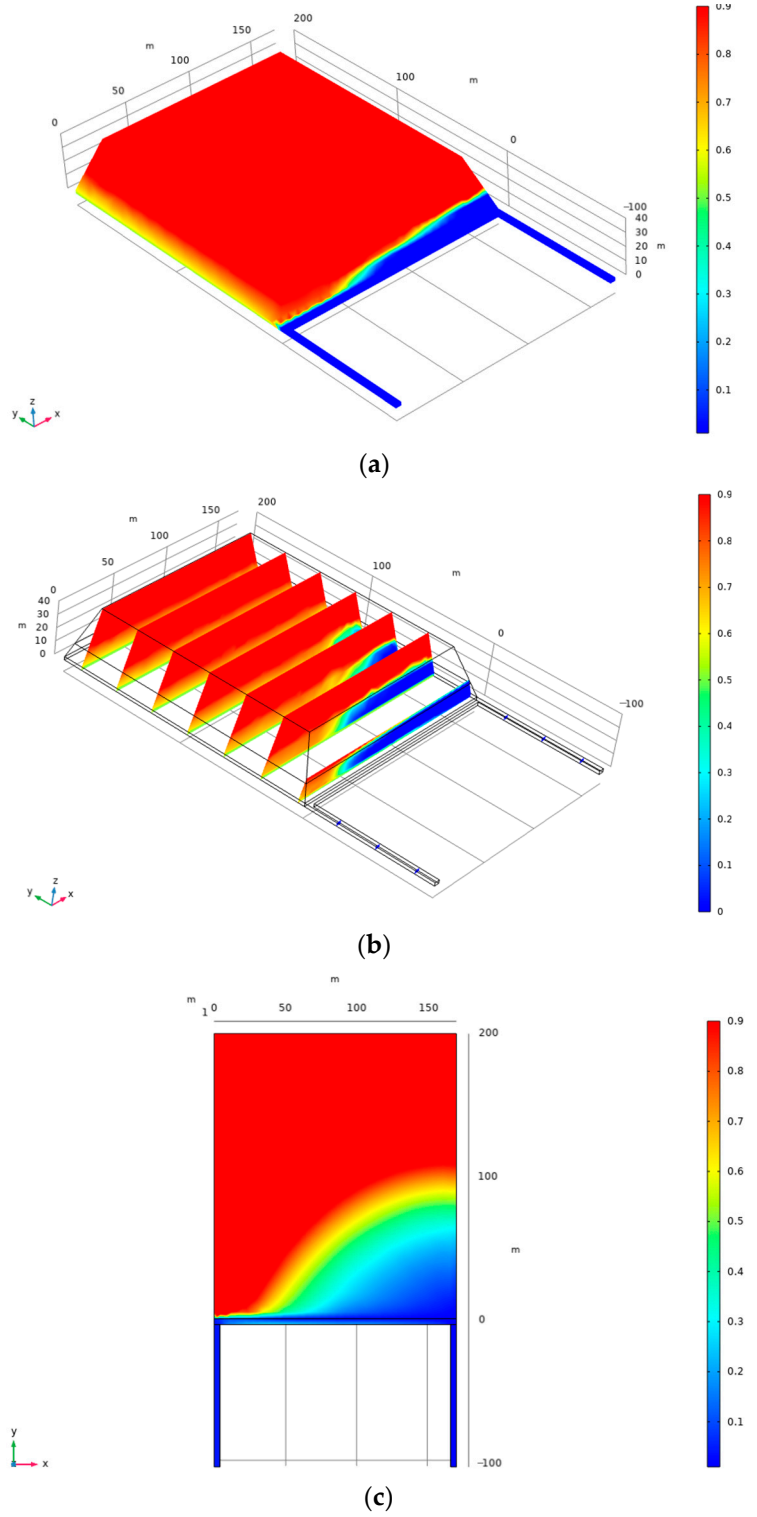

Figure 6. Three-dimensional distribution of gas in the goaf. (**a**) Overall diagram of the gas concentration distribution; (**b**) plane diagram of the gas concentration distribution; (**c**) bottom diagram of the gas concentration distribution.

According to Figure 5a, in the whole stope orientation of the working face and the goaf, the gas concentration on the side of the intake air roadway of the working face is the lowest, while the gas concentration at the top of the fractured zone of the goaf is the highest, reaching 89.7%.

According to Figure 5b, with the mining of the No. 1-2 coal seam, the pressure–relief gas of the No. 2 coal seam enters the working face and goaf of the No. 1-2 coal seam through the fracture under the action of a pressure gradient. At the position near the top cutting line of the return air side, the speed component of the air leakage airflow along the advancing direction of the working face is relatively large, and a gas accumulation area is formed at the upper corner of the return air roadway. The gas concentration is as high as 66.7%. Because the density of gas is lower than that of air, the gas in the No. 1-1 coal seam, which collapses to the goaf with mining, moves to the upper part of the goaf through the cracks in the overlying strata under the action of buoyancy. With the increase in the overlying strata, cracks available for gas migration are reduced, and gas floating resistance increases. A gas enrichment area with 83.6% concentration is formed at the boundary 10.8~24.1 m away from the roof of No. 1-2 coal seam.

According to Figure 5c, at the upper corner of the return air roadway, the disturbance of airflow is small, and the airflow leaking back through the goaf converges here. Therefore, the upper corner of the working surface is the key area for preventing gas accumulation.

According to the above analysis, with the mining of the No. 1-2 coal seam, No. 1-1 and No. 2 coal seams are all affected and experience the pressure–relief stage. Therefore, the final hole of the gas extraction hole should be arranged in the gas enrichment area of the gas-conducting fracture zone and the accumulation position near the upper corner of the return air roadway.

4. Optimization Design of Pressure–Relief Gas Drainage by Mining

The breaking of key strata in overlying strata plays a major role in the evolution of mining-induced fractures; this is the main factor affecting gas migration and enrichment under the conditions of short-distance seam mining. The layout position of pressure–relief gas drainage holes in short-distance seam groups should be combined with the evolution law of key overburden strata.

4.1. Layers of Pressure–Relief Gas Drainage Holes in the Short-Distance Coal Seam Group

Reasonable arrangement of drainage holes is the key to achieving the accurate extraction of pressure-relieved gas in the adjacent layer. The spatial arrangement position of the pressure–relief gas extraction hole determines the effect of pressure-relieved gas extraction in the short-distance seam group mining. From the "three zones" of pressure-relieved migration in short-distance seam group mining, the gas-conducting fracture zone is greatly affected by mining; the secondary fractures and gas migration channels are the most developed; and the pressure–relief gas migration is active, which is the main area of pressure–relief gas drainage. Therefore, the arrangement of the pressure–relief gas drainage holes in the short-distance coal seam group is the gas conducting fracture zone area, that is, the space within the maximum development height of the caving zone to the maximum development height of the gas-conducting fracture zone. Therefore, the arrangement horizon of pressure–relief gas drainage holes can be expressed according to Formula (4):

$$h_m < h < h_g \quad (4)$$

h_m—height of the caving zone, m;
h—vertical height of the coal seam roof of the pressure–relief gas drainage hole distance mining layer, m;
h_g—height of gas conducting fracture zone, m.

The height of caving zone h_m is related to the unidirectional compressive strength of overburden strata R_c [28,29]. When R_c < 10 MPa, h_m is calculated according to Formula (5);

when 10 MPa < R_c < 20 MPa, h_m is calculated according to Formula (6); when 20 MPa < R_c < 40 MPa, h_m is calculated according to Formula (7); when 40 MPa < R_c < 80 MPa, h_m is calculated according to Formula (8) [30].

$$h_m = \frac{100M}{7.0M+63}+1.2 \quad (5)$$

$$h_m = \frac{100M}{6.2M+32}+1.5 \quad (6)$$

$$h_m = \frac{100M}{4.7M+19}+2.2 \quad (7)$$

$$h_m = \frac{100M}{2.1M+16}+2.5 \quad (8)$$

M—height of the mining layer, m.

The height of the gas-conducting fracture zone h_g is related to the height of the main key strata from the mining layer [31,32]. When the height of the main key strata from the mining layer is greater than (7~10)M, the mining height h_g is the height of the coal seam of the nearest key strata from the mining layer outside the 7–10 mining height. When the height of the main key stratum is less than (7~10)M, h_g is the top height of the bedrock.

4.2. Position of the Pressure–Relief Gas Drainage Hole in Short-Distance Coal Seam Group

In the gas-conducting fracture zone, the separation fractures and broken fractures are extremely developed. The pressure–relief gas of the coal and rock mass around the stope continues to flow to it and gathers into a gas enrichment zone under the action of airflow. This area is the best space for extracting pressure–relief gas from adjacent layers. Mastering the width of the "O"-ring fracture zone is the key to determining the position of the pressure–relief gas extraction hole. According to previous studies [33], the width of "O"-ring fracture zone in the gas-conducting fracture zone can be calculated according to Formulas (9) and (10):

$$W(M) = k_2 W'(M) \quad (9)$$

$$W'(M) = 0.011M^3 - 0.640M^2+10.220M+13.514. \quad (10)$$

$W(M)$—width of the "O" ring crack area, m;
k_2—constant is taken as 0.8~1.1. When the overburden is less and the mining depth is larger, a small value is taken; otherwise, a large value is taken;
$W'(M)$—average width of "O" ring, m;
M—height of the mining layer, m.

4.3. Optimized Design Scheme of Pressure–Relief Gas Collaborative Drainage in the Short-Distance Coal Seam Group

The cooperative extraction mode of pressure–relief gas in the short-distance coal seam group was established based on the "three zones" division of gas pressure–relief extraction in the short-distance coal seam group and the gas migration characteristics in the "O"-ring area of the gas-conducting fracture zone, as shown in Figure 7.

(1) Directional long drilling pressure–relief in the far field gas-conducting fracture zone is observed. The roof directional long drillings are arranged in the gas-conducting fracture zone. Under the action of negative pressure and airflow, the pressure–relief gas in the gas-conducting fracture zone was effectively intercepted for the first time and prevented the accumulation of gas in the upper corner. The spatial arrangement position of the pressure–relief gas drainage holes in the adjacent layers of the short-distance coal seam

group should be close to the return air roadway to avoid the stress recovery zone, and the horizontal distance should be calculated according to Formula (11):

$$HD = [h - (h_2 + h\cot\beta)\tan\alpha]\sin\alpha + \frac{h_2 + h\cot\beta}{\cos\alpha}. \quad (11)$$

HD—horizontal distance from the directional long borehole in the roof to the return air roadway, m;
h—vertical height of the pressure–relief gas drainage hole from the roof of the coal seam of the mining seam, m;
α—dip angle of the coal seam;
β—included angle between the lines connecting the fracture boundary, mining boundary, and the coal seam;
h_2—distance from the borehole to the outer boundary of the "O"-ring fracture zone, which can be taken as 0.5 *W(M)*, m.

(2) Extraction of staggered buried-pipe in the near field goaf was performed. The buried pipes were arranged in the staggered distance of the return air roadway to extract the pressure–relief gas in the gas emission zone of the goaf. The gas in the low gas accumulation area flowing to the working face due to the destruction of the integrity of the directional long borehole of the roof was intercepted twice, which effectively reduced gas emission in the goaf.

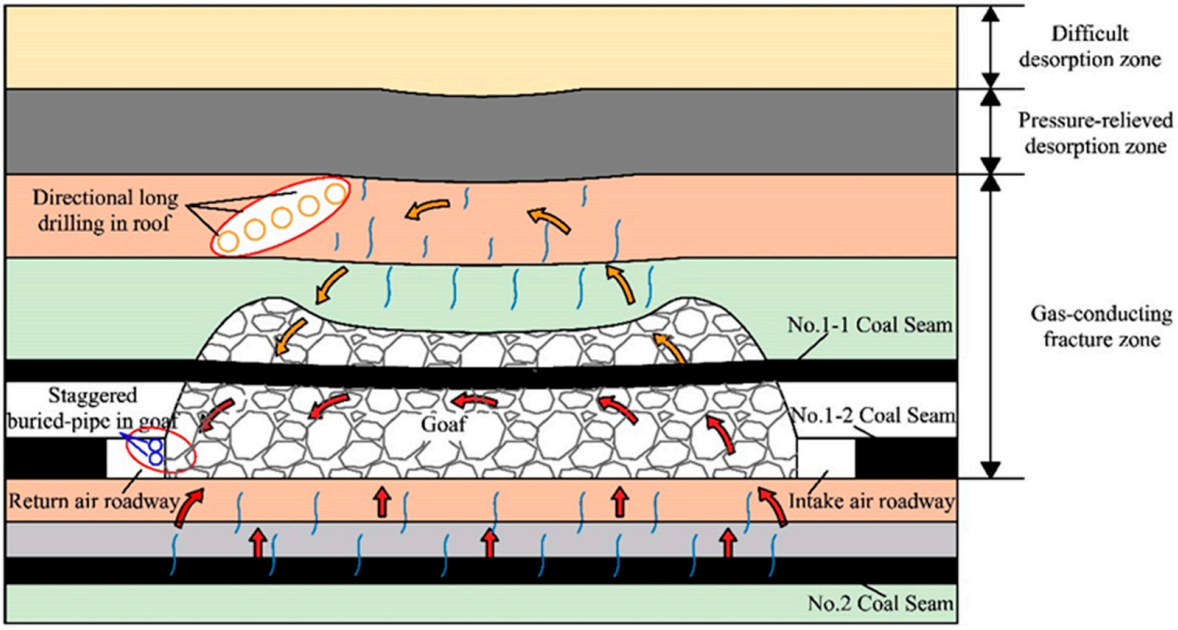

Figure 7. Schematic of layout of drill holes in collaborative extraction mode.

5. Engineering Application

5.1. Layering and Layout of Pressure–Relief Gas Drainage Holes

The physical and mechanical rock parameters were tested by coring detection within 30 m of the overburden coal and rock strata of the No. 1-2 coal seam roof. The compressive strength test is the ratio of the failure load to the bearing area of the standard specimen of coal or rock under uniaxial compression under laboratory conditions. The Brazilian splitting method was used to test the tensile strength; this experimental method determines the maximum tensile stress of a specimen by applying a radial compression line load to a solid cylinder specimen until failure. The elastic modulus was calculated according to the stress–strain curve [34]. The test results are shown in Table 2.

Table 2. Overburden physical and mechanical parameters of the No. 1-2 coal seam.

Lithology	Compressive Strength/MPa	Tensile Strength/MPa	Modulus of Elasticity/GPa
Coarse sandstone	76.3	4.8	7.9
Sandy mudstone	30.1	1.9	3.1
Medium and coarse sandstone	61.3	3.6	7.4
Sandy mudstone	34.8	2.4	3.2
Coal	14.7	1.3	1.1
Sandy mudstone	29.1	1.7	3.0
Coarse sandstone	76.4	4.1	8.1

According to Table 2, the compressive strength of the overlying coal stratum of the No. 1-2 coal seam is 20~80 MPa, which indicates medium-hard and hard strata. The mining thickness of the No.1-2 coal seam is 1.5 m, and the maximum h_m calculated by Formulas (7) and (8) is 10.3 m. According to the identification results for the key strata structure of the overburden of the working face combined with the calculation process, the overburden structure within 23.2 m above the roof of the 1211 working face is the gas-conducting fracture zone. The pressure–relief gas enrichment area is within 10.3~23.2 m of the roof of the 1211 working face, which is consistent with the numerical simulation results. According to Formula (4), the arrangement horizon of the pressure–relief gas drainage holes in the short-distance coal seam group mining is 10.3~23.2 m.

According to Formulas (9) and (10), the average width of the "O"-ring fracture area is 27.44 m. The average burial depth of the 1211 working face is 540 m, and there are many overlying strata. k_2 is 1.1, and the width of the "O"-ring fissure area in the gas-conducting fracture zone is 30.19 m.

5.2. Optimization Design of Pressure–Relief Gas Collaborative Drainage

To prevent the hidden danger of gas accumulation caused by a large amount of pressure–relief gas from the upper and lower adjacent seams pouring into the 1211 working face during the mining of the No. 1-2 coal seam, it is proposed that directional long drilling in the roof combined with the staggered buried-pipe in the goaf be used to drain the pressure–relief gas from the adjacent seams.

First, based on the above optimization design scheme of pressure–relief gas collaborative drainage, the height range of the directional long drilling in the roof should be arranged in the overlying strata above 10.3 m and below 23.2 m of the No. 1-2 coal seam roof. At the same time, considering the construction feasibility and the integrity of the final borehole, a reasonable layout horizon of the directional long borehole is in the sandy mudstone 14.7 m away from the roof working face to ensure a longer drainage time and higher drainage efficiency.

Second, based on the Formula (11) calculation for the arrangement of the pressure–relief gas drainage holes in the adjacent seam, the dip angle α of the coal seam was taken as 4°, the included angle β between the lines connecting the fracture boundary, mining boundary, and the coal seam was taken as 65°, and the distance from the borehole to the outer boundary of the "O"-ring was taken as 15.1 m. The horizontal distance between the directional long borehole in the roof of the 1211 working face and the return air roadway was calculated to be 20.5~27.5 m.

Based on the theoretical calculation and combined with the characteristics of the overlying coal and rock mass of the No. 1-2 coal seam roof, directional long drillings were performed in the No. 2 drilling field, 350 m away from the cutting hole of the 1211 return air roadway. Three main boreholes and two branch boreholes were arranged. The borehole spacing was 1.75 m, and the layer spacing was 2.0 m. The inclination of the opening was 9°, and the borehole aperture was 96 mm. The borehole construction parameters are shown in Table 3**.** After drilling was completed, the borehole was sealed by cement grouting; the negative pressure of drainage was 13 kPa.

Table 3. Parameters of roof directional long drillings.

Hole Number	Design Hole Depth/m	Hole Azimuth/°	Height of Final Hole to Roof of No. 1-2 Coal Seam/m	Horizontal Distance from the Final Hole to the Air Return Side/m
1#	380	275	15	20.50
1-2#	380	275	17	22.25
2#	380	278	19	24.00
2-2#	380	278	21	25.75
3#	380	281	23	27.50

Finally, to intercept the pressure–relief gas from the lower adjacent seam into the goaf for the second time, two pipelines with a diameter of 300 mm were arranged at the upper corner of the return air roadway at a staggered distance; one pipeline was located at a height of 1.1 m from the floor and a depth of 11.3 m into the goaf, and the other was arranged in parallel, at a height of 1.7 m from the floor and a depth of 20.8 m into the goaf. The negative pressure of the drainage was 20 kPa. The two drainage pipelines were arranged in a staggered manner in space and always located in the gas emission zone of the goaf; this ensured the continuity of drainage and effectively improved the effect of gas drainage. The borehole layout of pressure–relief gas cooperative extraction is shown in Figure 8.

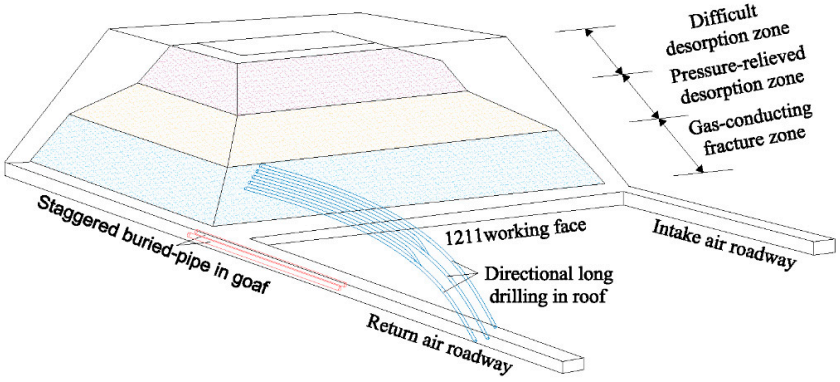

Figure 8. Layout of pressure–relief gas coordinated drainage boreholes.

5.3. Results and Analysis

Before the treatment measures were taken, the gas concentration in many working faces and upper corners of No. 1-2 coal seam often exceeded the limit, rendering normal operation and production impossible. In the working faces of No. 1201 and No. 1209, a control measure of buried-pipe in the goaf and directional drilling in the roof was adopted. The working face of No. 1211 adopted cooperative drainage technology. The gas concentration in the upper corner and the return air roadway with the above three control measures are reported in Table 4. The test site gas concentration was tested using a KG9701B low-density methane sensor. The test instrument is shown in Figure 9.

Table 4. Gas concentration in upper corner and return airway of working face when three kinds of control measures were adopted, respectively.

	1201 Working Face	1209 Working Face	1211 Working Face
The gas concentration in the upper corner/%	0.9	0.8	0.7
The gas concentration in the return air roadway/%	0.8	0.6	0.5



Item	Technical Parameter			
Measurement Range	(0.00 ~ 4.00) % CH_4			
Measurement Accuracy	Measurement Range	0.00 ~ 1.00% CH_4	1.00 ~ 2.00% CH_4	2.00 ~ 4.00% CH_4
	Intrinsic Error	±0.1% CH_4	±0.2% CH_4	±0.3% CH_4
Alarm Point	(0.50 ~ 2.50) % CH_4			
Response Speed	≤30 s			
Display Mode	Red digital-tube			
Alarm Mode	Intermittent sound and light alarm of diode (Sound intensity ≥ 80 dB, Light intensity: Visibility ≥ 20 m)			
Cut-off Point	0.50% CH_4, 0.75% CH_4, 1.00% CH_4, 1.25% CH_4, 1.50% CH_4			
Resume Point	0.40% CH_4, 0.65% CH_4, 0.90% CH_4, 1.15% CH_4, 1.40% CH_4			
Signal Transmission Distance	2 km			
Sampling Mode	Restricted diffusion			
Overall Dimension	(190×114×57) mm^3			
Weight	700 g			
Operating Environment	Temperature: (0 ℃~40 ℃) , Wind speed: (0 m/s~8 m/s)			
	Atmospheric pressure: (86 kPa~110 kPa) , Humidity: ≤ 98 %			

Figure 9. KG9701B low-density methane sensor and technical parameters.

From Table 4, compared with working faces 1201 and 1209, which only adopted one treatment measure, the gas concentration in the upper corner of the 1211 working face with cooperative drainage technology was reduced to less than 0.7%, and the gas concentration in the return air roadway was reduced to less than 0.5%. The governance effect was best. In order to better understand the situation of pressure–relief gas control, the gas volume fraction of the return air roadway and upper corner of the 1211 working face and the gas extraction volume in the drainage pipes were monitored on site during the mining period from May 5 to 11–15, 2020, as shown in Figure 10.

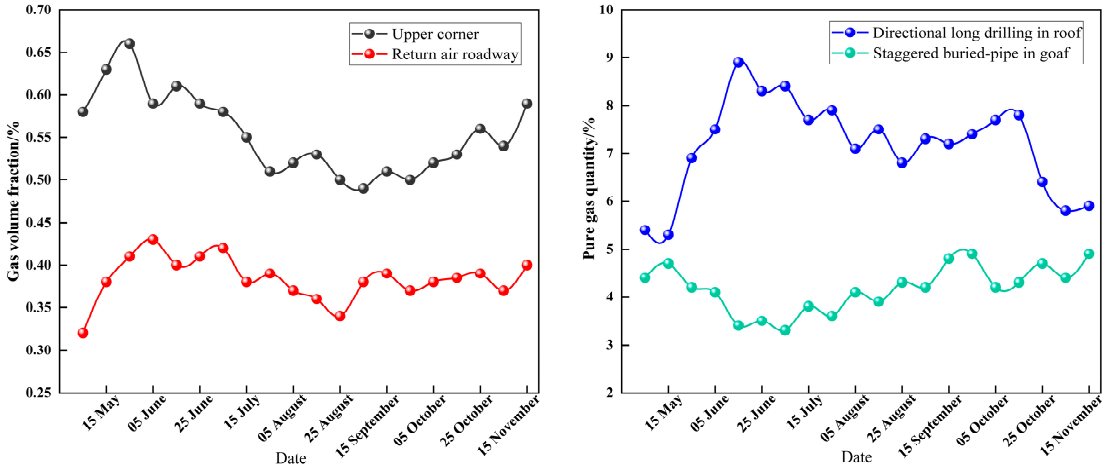

Figure 10. Investigation of cooperative extraction effect.

As can be seen in Figure 10, the average extraction volumes of the directional long drilling in the roof and the staggered buried-pipe in the goaf were 7.4 m^3/min and 4.8 m^3/min, and the average extraction concentrations were 73.2% and 5.7%, respectively. The average gas drainage rate of the collaborative drainage technology was 83.2%, which meets the requirement that the gas drainage rate of the working face should be greater than 40%. From further analysis, several tendencies can be observed in Figure 10.

First, in the initial stage of mining, because the fracture zone of the overlying coal and rock strata has not developed to the position of the directional long drilling in the roof, the

drainage effect is relatively poor, but, with the technical measures of staggered buried pipe drainage in the goaf, the volume fraction of the upper corner can still be stabilized below 0.7%.

Second, with the increase in mining distance, the directional drillings in the roof are located in the fracture zone, the drainage measures are implemented efficiently, and the drainage effect is remarkable.

Third, in the later stage of drainage, the integrity of directional long drilling is damaged by mining, and the drainage effect is slightly reduced.

6. Conclusions

(1) The law of gas enrichment of pressure–relief in the short-distance coal seam group was obtained. Under the influence of gas pressure gradient and buoyancy, a gas concentration enrichment zone was formed at a distance of 10.8–24.1 m from the boundary of the mining layer.

(2) The pressure–relief gas collaborative control technology mode, combining "directional drilling in the gas-conducting fractured zone + staggered buried-pipe in the goaf" was first proposed, and the layout parameters were optimized.

(3) The field test demonstrated that during the mining period of the working face, the average gas drainage rate was 83.2%, and the gas volume fraction in the upper corner was maintained below 0.7%; this indicates that cooperative gas extraction technology can greatly improve the efficiency of mining mineral resources and gas energy utilization in short-distance coal seam groups.

Author Contributions: Conceptualization, L.N.; methodology, A.Y.; software, L.N. and Z.H.; validation, L.N., A.Y. and Z.H.; formal analysis, L.N. and A.Y.; investigation, L.N., A.Y. and Z.H.; resources, L.N. and A.Y.; data curation, L.N. and A.Y.; writing-original draft preparation, L.N.; writing-review and editing, Z.H.; visualization, L.N. and A.Y. supervision, Z.H.; All authors have read and agreed to the published version of the manuscript.

Funding: The research was funded by the [University-level general projects of Anhui University of science and technology] grant number [xjyb2020-02], the [National Natural Science Foundation of China] grant number [52104073], the [Open Fund for Key Laboratory of Industrial Dust Prevention and Control & Occupational Health and Safety Ministry of Education] grant number [EK20211001].

Institutional Review Board Statement: Not applicable.

Informed Consent Statement: Not applicable.

Data Availability Statement: All datasets are publicly available.

Acknowledgments: Special thanks to Jie Gao for his help in the research background and methods of this article.

Conflicts of Interest: The authors declare no conflict of interest.

References

1. Zhao, P.; Wang, J.; Li, S.; Li, H.; Qin, L.; Lin, H.; Shu, C.-M.; Bin, L.; Jia, Y.; Wei, Z.; et al. Effects of Recovery Ratio on the Fracture Evolution of the Overburden Pressure-Relief Gas Migration Channel for a Fully Mechanized Working Face. *Nat. Resour. Res.* **2022**, *31*, 1011–1026. [CrossRef]
2. Xu, C.; Wang, K.; Li, X.M.; Yuan, L.; Zhao, C.Y.; Guo, H.J. Collaborative gas drainage technology of high and low level roadways in highly-gassy coal seam mining. *Fuel* **2022**, *323*, 13. [CrossRef]
3. Zhang, R.; Cheng, Y.P.; Yuan, L.; Zhou, H.X.; Wang, L.; Zhao, W. Enhancement of gas drainage efficiency in a special thick coal seam through hydraulic flushing. *Int. J. Rock Mech. Min. Sci.* **2019**, *124*, 12. [CrossRef]
4. Yuan, A.Y.; Wang, P.; Li, Y. Movement laws of overlying strata and prevention measures of dynamic disasters under deep adjacent coal seam group with high gas. *Geomat. Nat. Hazards Risk* **2020**, *11*, 2339–2359. [CrossRef]
5. Li, L.; Wu, G.; Liu, Q. Study on Overburden Movement and Fissure Evolution Law of Protective Layer Mining in Shallow Coal Seam. *Energies* **2022**, *15*, 1831. [CrossRef]
6. Shang, Z.; Wang, H.F.; Cheng, Y.P.; Li, B.; Dong, J.; Liu, Q.Q. Optimal selection of coal seam pressure-relief gas extraction technologies: A typical case of the Panyi Coal Mine, Huainan coalfield, China. *Energy Sources Part A Recovery Util. Environ. Eff.* **2022**, *44*, 1105–1125. [CrossRef]

7. Li, Q.; Wu, G.Y.; Kong, D.Z. Study on Stability of Stope Surrounding Rock under Repeated Mining in Close-Distance Coal Seams. *Geofluids* **2022**, *2022*, 9630942. [CrossRef]
8. He, F.L.; Li, L.; Lv, K.; Qin, B.B.; Xu, X.H.; Ma, Q.; Chen, Y.Q. Study on Evolution of Front Abutment Pressure at Working Face in Repeated Mining of Close-Distance Coal Seams. *Sustainability* **2022**, *14*, 12399. [CrossRef]
9. Yuan, A.Y.; Huang, C.H.; Hou, J.L.; Zhang, Z.M.; Pan, W.H.; Duan, L.; Wu, Q.S. A Study of the Solid-Liquid-Gas Three-Phase Coupling Relationship of Coal, Water and Gas. *Geofluids* **2020**, *2020*, 8882114. [CrossRef]
10. Li, Y.; Ren, Y.Q.; Peng, S.S.; Cheng, H.Z.; Wang, N.; Luo, J.B. Measurement of overburden failure zones in close-multiple coal seams mining. *Int. J. Min. Sci. Technol.* **2021**, *31*, 43–50. [CrossRef]
11. Cui, F.; Jia, C.; Lai, X.P.; Yang, Y.B.; Dong, S. Study on the Law of Fracture Evolution under Repeated Mining of Close-Distance Coal Seams. *Energies* **2020**, *13*, 6064. [CrossRef]
12. Yang, K.; Fu, Q.; Liu, Q.J.; He, X.; Lyu, X. Evolution of Mining-Induced Stress in Downward Mining of Short-Distance Multiseam. *Geofluids* **2022**, *2022*, 3305734. [CrossRef]
13. Wang, F.T.; Zhang, C.; Liang, N.N. Gas Permeability Evolution Mechanism and Comprehensive Gas Drainage Technology for Thin Coal Seam Mining. *Energies* **2017**, *10*, 1382. [CrossRef]
14. Cheng, H.; Zhao, H.B.; Ji, D.L.; Cui, L.Y. Evolution of mining stress field and the control technology of stress relief gas in close distance coal seam. *Energy Explor. Exploit.* **2022**, *40*, 1573–1588. [CrossRef]
15. Gao, Y.B.; Lin, B.Q.; Yang, W.; Li, Z.W.; Pang, Y.; Li, H. Drilling large diameter cross-measure boreholes to improve gas drainage in highly gassy soft coal seams. *J. Nat. Gas Sci. Eng.* **2015**, *26*, 193–204. [CrossRef]
16. Lu, T.K.; Wang, Z.F.; Yang, H.M.; Yuan, P.J.; Han, Y.B.; Sun, X.M. Improvement of coal seam gas drainage by under-panel cross-strata stimulation using highly pressurized gas. *Int. J. Rock Mech. Min. Sci.* **2015**, *77*, 300–312. [CrossRef]
17. Gao, M.Z.; Zhang, Z.L.; Yin, X.G.; Xu, C.; Liu, Q.; Chen, H.L. The Location Optimum and Permeability-Enhancing Effect of a Low-Level Shield Rock Roadway. *Rock Mech. Rock Eng.* **2018**, *51*, 2935–2948. [CrossRef]
18. Hu, G.Z.; Xu, J.L.; Ren, T.; Gu, C.X.; Qin, W.; Wang, Z.W. Adjacent seam pressure-relief gas drainage technique based on ground movement for initial mining phase of longwall face. *Int. J. Rock Mech. Min. Sci.* **2015**, *77*, 237–245. [CrossRef]
19. An, F.H.; Wang, Z.F.; Yang, H.M.; Yang, S.Y.; Pan, F.M.; Chen, T.; Xie, C. Application of directional boreholes for gas drainage of adjacent seams. *Int. J. Rock Mech. Min. Sci.* **2016**, *90*, 35–42. [CrossRef]
20. Duan, H.J.; Wang, Y.; Xiao, Q.; Wang, J.L.; Peng, D. Gas extraction technology and application of near horizontal high directional drilling. *Energy Rep.* **2022**, *8*, 1326–1333. [CrossRef]
21. Gharehdash, S.; Sainsbury, B.A.L.; Barzegar, M.; Palymskiy, I.B.; Fomin, P.A. Topology and hydraulic permeability estimation of explosively created fractures through regular cylindrical pore network models. *Eng. Comput.* **2021**, *38*, 2312–2353. [CrossRef]
22. Zheng, X.G.; Feng, X.W.; Zhang, N.; Liu, J.Z.; Zhang, L. Fissures Evolution Law and Gas Drainage Characteristics of Remote Decompressed Mining. *Disaster Adv.* **2013**, *6*, 164–176.
23. Ye, Q.; Wang, G.; Jia, Z.Z.; Zheng, C.S.; Wang, W.J. Similarity simulation of mining-crack-evolution characteristics of overburden strata in deep coal mining with large dip. *J. Pet. Sci. Eng.* **2018**, *165*, 477–487. [CrossRef]
24. Zhang, C.L.; Zhang, Y.; Zuo, J.P.; Gao, S.Y. Fracture Pattern of Overlying Strata in Multiple Coal Seam Mining in a Physical Model Vis-a-vis MATLAB Analysis and Geological Radar. *Min. Metall. Explor.* **2021**, *38*, 897–911. [CrossRef]
25. Xu, P.Y.; Li, S.G.; Lin, H.F.; Ding, Y.; Shuang, H.Q.; Liu, S.B.; Tian, Y. Fractal Characterization of Pressure-Relief Gas Permeability Evolution in a Mining Fracture Network. *Energies* **2021**, *14*, 7031. [CrossRef]
26. Zhu, Z.H.; Feng, T.; Yuan, Z.G.; Xie, D.H.; Chen, W. Solid-Gas Coupling Model for Coal-Rock Mass Deformation and Pressure Relief Gas Flow in Protection Layer Mining. *Adv. Civ. Eng.* **2018**, *2018*, 5162628. [CrossRef]
27. Liang, T.; Liu, X.L.; Wang, S.J.; Wang, E.Z.; Li, Q.S. Study on the Fractal Characteristics of Fracture Network Evolution Induced by Mining. *Adv. Civ. Eng.* **2018**, *2018*, 9589364. [CrossRef]
28. Cao, J.; Li, W.P. Numerical simulation of gas migration into mining-induced fracture network in the goaf. *Int. J. Min. Sci. Technol.* **2017**, *27*, 681–685. [CrossRef]
29. Du, F.; Jiao, K.; Ma, Z.Y. Influence of Key Strata on the Gas Downward Leakage Law in Dual-System of Coal Seam. *Geofluids* **2020**, *2020*, 8897260. [CrossRef]
30. Hu, G.J.; Ma, G. Size effect of parallel-joint spacing on uniaxial compressive strength of rock. *PLoS ONE* **2021**, *16*, e0257245. [CrossRef]
31. Wang, F.; Xu, J.L.; Chen, S.J.; Ren, M.Z. Method to Predict the Height of the Water Conducting Fractured Zone Based on Bearing Structures in the Overlying Strata. *Mine Water Environ.* **2019**, *38*, 767–779. [CrossRef]
32. Miao, X.X.; Cui, X.M.; Wang, J.A.; Xu, J.L. The height of fractured water-conducting zone in undermined rock strata. *Eng. Geol.* **2011**, *120*, 32–39. [CrossRef]
33. Xie, S.R.; Zhao, Y.J.; Zhang, S.B.; Yang, H.Z.; Xiao, D.C.; Tian, C.Y. Mechanism and experiment of substituting high drainage roadway with directional long drilling group to extract pressure-relief gas. *J. Cent. South Univ.* **2012**, *19*, 2591–2597. [CrossRef]
34. Tatone, B.S.A.; Abdelaziz, A.; Grasselli, G. Novel Mechanical Classification Method of Rock Based on the Uniaxial Compressive Strength and Brazilian Disc Strength. *Rock Mech. Rock Eng.* **2022**, *55*, 2503–2507. [CrossRef]

Disclaimer/Publisher's Note: The statements, opinions and data contained in all publications are solely those of the individual author(s) and contributor(s) and not of MDPI and/or the editor(s). MDPI and/or the editor(s) disclaim responsibility for any injury to people or property resulting from any ideas, methods, instructions or products referred to in the content.